

Quantum Degenerate Majorana Zero Modes in Two-Dimensional Continuous Space

Yen-Ting Lin¹, Ching-Yu Huang², Hao Lee¹, Daw-Wei Wang^{1,2}

¹ *Physics Department, National Tsing Hua University, Hsinchu, Taiwan*

² *Physics Division, National Center for Theoretical Sciences, Hsinchu, Taiwan*

(Dated: December 14, 2024)

We investigate the topological properties of spin polarized fermionic polar molecules loaded in a multi-layer structure with the electric dipole moment polarized to the normal direction by an external electric field. When fermions are paired by attractive inter-layer interaction, unpaired Majorana Zero Modes (MZMs) can be macroscopically generated in the 2D surface layers, if their in-plane kinetic energy satisfies a certain condition. We show that the resulting topological state is composed by 1D effective Kitaev ladders in momentum space, which are of BDI class characterized by the winding number \mathbb{Z} . We further calculate the entanglement entropy, entanglement spectrum, and the critical temperature for realizing such MZMs, and then discuss the signature for observing such 2D quantum degenerate MZMs in the time-of-flight experiments.

Introduction: A Majorana fermion (MF) is known to be its own antiparticle [1], as a hypothesis in theoretical particle physics. In condensed matter systems, a MF can appear as a localized edge state, reflecting the topological order (TO) in the bulk of system. It is known that systems of topological order can be classified into intrinsic TO or symmetry-protected topological (SPT) order: the latter is robust against local perturbations for a given on-site symmetries [2]. Ground states of nontrivial SPT phases cannot be continuously connected to trivial product states without either closing the gap or breaking the protecting symmetry [3].

One of the mostly studied TO phase is proposed by Kitaev [4] for one-dimensional (1D) p -wave superconductor. The Majorana zero mode (MZM) of such system may be applied for quantum computation through braiding, and certain experimental signature has been proposed in an ordinary s -wave superconducting wire with strong spin-orbital coupling through proximity effect [5–13] or even in systems of ultracold atoms [14–17]. However non-ambiguous evidence is still lacking probably due to the poor signal-to-noise ratio for a localized MZM. Recently, some extensions of Kitaev’s 1D model by including inter-chain tunneling [18], dimerization [19], and long-ranged pairing [20, 21] have also been proposed.

In the systems of quantum gases, such inter-site pairing between fermions can be provided by the long-ranged dipolar interactions between polar molecules [22–25] or neutral atoms with a large magnetic moment [26–28]. Since the inelastic scattering between polar molecules can be well suppressed by aligning dipole moments normal to the two-dimensional (2D) plane with a strong transverse confinement [29–31], many exotic ground states have been predicted in a 2D layer [32–45] or in a bi/multi-layer structure [43–48].

In this paper, we proposed that quantum degenerate MZMs can exist in a 2D continuous space, when spin polarized fermionic polar molecules are paired in a stack of multi-layer structure (Fig. 1(a)) through their dipolar interaction. Within the meanfield approximation, the system is equivalent to an ensemble of Kitaev ladders (see Fig. 1(b)), labelled by a pair of in-plane momenta,

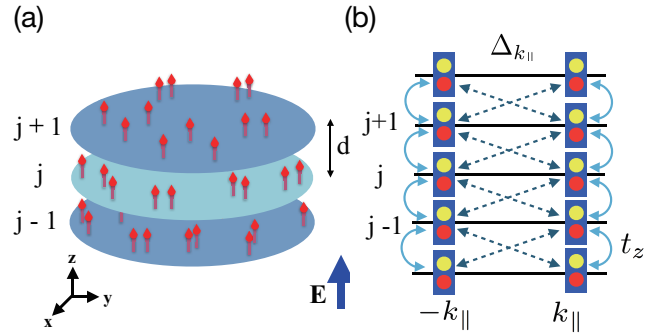


FIG. 1: (a) Multi-layer structure for identical fermionic polar molecules loaded into a deep 1D optical lattice. The electric dipole moment (arrows) is aligned to the normal (z) direction by the external field. (b) Effective Kitaev ladder in momentum space (see Eq. (2)), where fermions (rectangular boxes) in each “site” can be decomposed into two MFs (circles, see the text). Two unpaired MZM can be found at the end of ladders if Eq. (5) is satisfied. Double-sided arrows of dashed/solid lines indicate inter-layer pairing/hopping respectively.

($\mathbf{k}_{\parallel}, -\mathbf{k}_{\parallel}$). We show that the ground state has a TO in the BDI class, characterized by the \mathbb{Z} index as a nontrivial winding number, when some condition is satisfied (see Eq. (5)). We further calculate the entanglement entropy as well as entanglement spectrum to confirm such topological phases. From experimental point of view, the degenerate MZMs can be observed through the additional short period interference fringes between MZMs in the two end in the time-of-flight experiment. The critical temperature is estimated (by self-consistently solving the gap equation) to be about one-tenth of the in-plane Fermi energy. Our results suggest a new system to investigate quantum many-body properties of non-Abelian anyons in a 2D continuous space.

System Description and Effective Hamiltonian: The system setup is illustrated in Fig. 1(a), where identical (spin polarized) fermionic polar molecules are loaded into a stack of 2D layers with interlayer spacing d and tunneling amplitude t_z . The electric dipole moment is polarized

perpendicular to the layer by the external field, leading to a repulsive intra-layer interaction and an attractive inter-layer interaction between molecules. The former just renormalizes the effective mass and the chemical potential [43, 50] within Landau-Fermi liquid theory, and therefore can be neglected first. Since such a system is effective three-dimensional, the meanfield BCS theory due to the inter-layer attractive interaction can be well justified. The resulting Bogoliubov-de Gennes (BdG) Hamiltonians becomes $H_{\text{BdG}} = \sum_{\mathbf{k}_{\parallel}} H_{\mathbf{k}_{\parallel}}$, where

$$H_{\mathbf{k}_{\parallel}} = \sum_{j=1}^L \left(\frac{\mathbf{k}_{\parallel}^2}{2m} - \mu \right) c_{\mathbf{k}_{\parallel},j}^{\dagger} c_{\mathbf{k}_{\parallel},j} \quad (1)$$

$$- \sum_{j=1}^{L-1} \left[t_z c_{\mathbf{k}_{\parallel},j}^{\dagger} c_{\mathbf{k}_{\parallel},j+1} + \Delta_{\mathbf{k}_{\parallel}} c_{\mathbf{k}_{\parallel},j}^{\dagger} c_{-\mathbf{k}_{\parallel},j+1}^{\dagger} + \text{h.c.} \right].$$

Here $c_{\mathbf{k}_{\parallel},j}$ is field operator of the j th layer with in-plane momentum, \mathbf{k}_{\parallel} ; μ and m are chemical potential and molecule mass respectively. $\Delta_{\mathbf{k}_{\parallel}} = \Delta_{-\mathbf{k}_{\parallel}}$ is the gap function between nearest neighboring layers. One can include longer-ranged pairing due to the dipolar interaction, but it will not change the nature of the TO as has been shown in Ref. [21].

We can find that $H_{\mathbf{k}_{\parallel}}^{\text{ladd}} \equiv H_{\mathbf{k}_{\parallel}} + H_{-\mathbf{k}_{\parallel}}$ forms a closed Kitaev ladder in momentum space, where the TO (if exists) is protected by time-reversal, particle-hole, and chiral symmetries at the same time, and hence belongs to BDI class of Altland-Zirnbauer classification [2]. Note that we can effectively consider the fermionic system to be time-reversal symmetric if initially preparing all molecules in the same hyperfine state (i.e. spin polarized [49]). Exchange interaction between these hyperfine states can be so weak that spin states are frozen (i.e. spin polarized) during the system holding time.

Majarona Fermions at the Edge: To see how MFs may appear in $H_{\mathbf{k}_{\parallel}}^{\text{ladd}}$, we first consider a special case when $\mathbf{k}_{\parallel}^2/2m - \mu = 0$ and $\Delta_{\mathbf{k}_{\parallel}} = t_z$. MFs in momentum space can then be defined: $\gamma_{\mathbf{k}_{\parallel},j}^{(1)} \equiv c_{\mathbf{k}_{\parallel},j} + c_{-\mathbf{k}_{\parallel},j}^{\dagger}$ and $\gamma_{\mathbf{k}_{\parallel},j}^{(2)} \equiv -i(c_{\mathbf{k}_{\parallel},j} - c_{-\mathbf{k}_{\parallel},j}^{\dagger})$, with the anti-commutation relations, $\{\gamma_{j,\mathbf{k}}^{(a)}, \gamma_{j',\mathbf{k}'}^{(b)}\} = 2\delta_{j,j'}\delta_{a,b}\delta_{\mathbf{k},\mathbf{k}'}$ ($a, b = 1, 2$). After a some algebra, we obtain (see Supplemental Materials)

$$H_{\mathbf{k}_{\parallel}}^{\text{ladd}} = it_z \sum_{j=1}^{L-1} \left(\gamma_{\mathbf{k}_{\parallel},j}^{(2)} \gamma_{-\mathbf{k}_{\parallel},j+1}^{(1)} + \gamma_{-\mathbf{k}_{\parallel},j}^{(2)} \gamma_{\mathbf{k}_{\parallel},j+1}^{(1)} \right), \quad (2)$$

where the ladder becomes two decoupled chains with two MFs missed at each end (see Fig. 1(b)): $\gamma_{\pm\mathbf{k}_{\parallel},1}^{(1)}$ for the bottom layer ($j = 1$), and $\gamma_{\pm\mathbf{k}_{\parallel},L}^{(2)}$ for the top layer ($j = L$). One can easily construct two "real" MFs in each layer by defining $\bar{\gamma}_{\pm,k}^{(a)} = (\pm 1)^{\frac{1}{2}} (\gamma_{\mathbf{k}_{\parallel}}^{(a)} \pm \gamma_{-\mathbf{k}_{\parallel}}^{(a)})$, which is its own anti-particle: $(\bar{\gamma}_{\pm,k}^{(a)})^{\dagger} = \bar{\gamma}_{\pm,k}^{(a)}$ with $k \equiv |\mathbf{k}_{\parallel}|$ and $a = 1, 2$.

From above analysis, we can find three important properties on these MZMs: (1) As discussed in Kitaev's seminar work [4], even for ladders with $k_{\parallel}^2/2m \neq \mu$ or $\Delta_{\mathbf{k}_{\parallel}} \neq t_z$, we can still diagonalize $H_{\mathbf{k}_{\parallel}}^{\text{ladd}}$ by introducing new MFs, $\tilde{\gamma}_{\mathbf{k}_{\parallel},l}^{(a)}$, which is a linearly combination of $\gamma_{\mathbf{k}_{\parallel},j}^{(a)}$ ($a = 1, 2$), and satisfies $\{\tilde{\gamma}_{\mathbf{k}_{\parallel},l}^{(a)}, \tilde{\gamma}_{\mathbf{k}_{\parallel},l'}^{(b)}\} = 2\delta_{l,l'}\delta_{a,b}\delta_{\mathbf{k}_{\parallel},\mathbf{k}'_{\parallel}}$. A localized MZM, $\tilde{\gamma}_{\pm\mathbf{k}_{\parallel},l=1/L}^{(1)}$ near the bottom/top layer (now the index l is not layer index) can be still retained when a certain condition is satisfied (see Eq. (5) below). (2) When applying a single particle perturbation, say $H_1 = i \sum_{\mathbf{k},\mathbf{k}'} A(\mathbf{k}_{\parallel},\mathbf{k}'_{\parallel}) \tilde{\gamma}_{\mathbf{k}_{\parallel},1}^{(1)} \tilde{\gamma}_{\mathbf{k}'_{\parallel},1}^{(1)}$, we can show that $A(\mathbf{k}_{\parallel},\mathbf{k}'_{\parallel}) = 0$ if H_1 has to satisfy time-reversal symmetry (TRS) (see Supplemental Materials for details). This results from the fact that all $\tilde{\gamma}_{\mathbf{k}_{\parallel},1}^{(1)}$ keep the same phase with respect to time-reversal transformation, and therefore cannot be re-combined to be a Dirac fermion. As a result, the topologic order we observed, characterized by MZMs in the surface layers, should be stable and protected by TRS at least in the single particle level, even these MFs are overlapped in a continuous space. (3) The Kitaev ladder we discussed above is very similar to a coupled Kitaev chains in real space (see Ref. [18] for example). However, the pairing function of different chains can be in principle of different phases, making different types of MFs, $\tilde{\gamma}^{(1)}$ or $\tilde{\gamma}^{(2)}$, mixed at the same edge and hence unstable by perturbation. However, the inter-layer pairing shown in Eq. (2) is dominated by s -wave pairing (i.e. $\Delta_{\mathbf{k}_{\parallel}}$ is of the same phase for all \mathbf{k}_{\parallel}) due to the attractive inter-layer dipolar interaction (the 3D gap function is still anti-symmetric along the chain direction). This explains why our MFs must be of the same type (same eigenvalue with time-reversal) in the same layer, ensuring the stability of the topological order even when a local disorder or a trapping potential is included.

Condition for Topological Order: To investigate the topological properties in the bulk system, we apply Fourier transform on the Hamiltonian (Eq. (2)) with the periodic boundary condition. Defining Nambu spinor, $C_{k_{\parallel},k_z} = [c_{k_{\parallel},k_z}, c_{-k_{\parallel},-k_z}^{\dagger}]^T$, we obtain,

$$H_{\text{BdG}} = \sum_{k_{\parallel}} \sum_{k_z} C_{k_{\parallel},k_z}^{\dagger} \begin{bmatrix} \xi_{\mathbf{k}} & -\tilde{\Delta}_{\mathbf{k}} \\ -\tilde{\Delta}_{\mathbf{k}}^* & -\xi_{\mathbf{k}} \end{bmatrix} C_{k_{\parallel},k_z}, \quad (3)$$

where $\xi_{\mathbf{k}} \equiv \frac{\mathbf{k}_{\parallel}^2}{2m} - \mu - 2t_z \cos(k_z)$. Note that we define 3D momentum $\mathbf{k} \equiv (\mathbf{k}_{\parallel}, k_z)$ and 3D gap function $\tilde{\Delta}_{\mathbf{k}} \equiv 2i\Delta_{\mathbf{k}_{\parallel}} \sin(k_z d)$ for the convenience of later discussion. The BdG Hamiltonian can be unitary transformed to off-diagonal, $H_{\text{BdG}} = \frac{i}{4} \sum_{\mathbf{k}} \Gamma_{\mathbf{k}}^{\dagger} \begin{bmatrix} 0 & v_{\mathbf{k}} \\ v_{\mathbf{k}}^{\dagger} & 0 \end{bmatrix} \Gamma_{\mathbf{k}}$, with $v_{\mathbf{k}} \equiv \xi_{\mathbf{k}} + \frac{1}{2}(\tilde{\Delta}_{\mathbf{k}}^* - \tilde{\Delta}_{\mathbf{k}}) = \xi_{\mathbf{k}} - 2i\Delta_{\mathbf{k}_{\parallel}} \sin(k_z d)$ and $\Gamma_{\mathbf{k}} \equiv [c_{\mathbf{k}} + c_{-\mathbf{k}}^{\dagger}, -ic_{\mathbf{k}} + ic_{-\mathbf{k}}^{\dagger}]^T$. The winding number can

be calculated as following [18]:

$$W_{\mathbf{k}_{\parallel}} \equiv \int_{-\pi/d}^{\pi/d} \frac{dk_z}{2\pi} \partial_{k_z} \theta_{\mathbf{k}_{\parallel}, k_z}$$

$$= \frac{J_-}{2} \oint \frac{dz}{2\pi i} \frac{z^2 + 2J_+ z + 1}{J_1 J_2 [(z-Z_1)(z-Z_2)(z-Z_3)(z-Z_4)]} \quad (4)$$

where $\mu_{\mathbf{k}_{\parallel}} \equiv \mu - \frac{\mathbf{k}_{\parallel}^2}{2m}$, $J_1 = \frac{t_z + \Delta_{\mathbf{k}_{\parallel}}}{\mu_{\mathbf{k}_{\parallel}}}$, $J_2 = \frac{t_z - \Delta_{\mathbf{k}_{\parallel}}}{\mu_{\mathbf{k}_{\parallel}}}$, and $J_{\pm} = J_1 \pm J_2$. Four poles of the integrand are given as $Z_{1,2} = \frac{-1 \pm \sqrt{1-4J_1 J_2}}{2J_1}$ and $Z_{3,4} = \frac{-1 \pm \sqrt{1-4J_1 J_2}}{2J_2}$ respectively. (see Supplemental Materials for details). One can find that $W_{\mathbf{k}_{\parallel}}$ become nonzero (i.e. topological non-trivial) when the following condition is satisfied:

$$|\mu_{\mathbf{k}_{\parallel}}| = \left| \mu - \frac{\mathbf{k}_{\parallel}^2}{2m} \right| < 2t_z, \quad (5)$$

which is independent of the gap function as expected.

This result shows that the TO appears when the in-plane kinetic energy is within a certain range: $\text{Max}(0, \mu - 2t_z) < \mathbf{k}_{\parallel}^2/2m < \mu + 2t_z$. In the 3D limit of large t_z , ladders of all in-plane momenta can be topological, while in the 2D limit of small t_z , only those near Fermi surface are topological. Assuming the gap is so small that only states below Fermi energy, $E_F \equiv k_F^2/2m = \mu$, are occupied, we can show that the ratio of the total number of unpaired MFs to average number of particles in the surface layers is given by $\eta_{\text{plane}} = \text{Min}(1, 2t_z/\mu)$ (see Supplementary Material).

Entanglement spectrum: Besides of the winding number, a topological phase can be also characterized by the quantum entanglement between the subsystem and the environment [51–53]. In short, given a ground state wave function $|\Psi\rangle$, one can calculate the reduced density matrix, ρ_A , for a subsystem A by tracing over the environment (see Fig. 2(a)). The eigenvalues λ_{α} of the reduced density matrix is so-called “entanglement spectrum” [52], which carries nonlocal information and has been applied for calculating Berry phase and zero-energy edge states [54]. For example, the degeneracy of the entanglement spectrum has recently implemented to characterize the topological orders for some 2D quantum Hall states [52] and for some 1D SPT phases [53].

For 1D Kitaev model, λ_{α} is given by the eigenvalues of the block Green’s function matrix, i.e., $G_{\mathbf{k}_{\parallel}, i, j} \equiv \langle c_{\mathbf{k}_{\parallel}, i} c_{\mathbf{k}_{\parallel}, j}^{\dagger} \rangle$ with the layer indices i and j inside the subsystem A . In Ref. [54, 55], it has been shown that the zero energy mode of the 1D Kitaev model corresponds to the degeneracy of $\lambda_{\alpha} = 1/2$ in the entanglement spectrum, i.e. the pair of zero modes at the two ends of Kitaev’s chain contribute the maximal entanglement between the subsystem A and environment.

Besides of entanglement spectrum, a topological phase transition can be also identified by the entanglement entropy of the subsystem (given by $S_A = -\text{Tr} \rho_A \log \rho_A$)

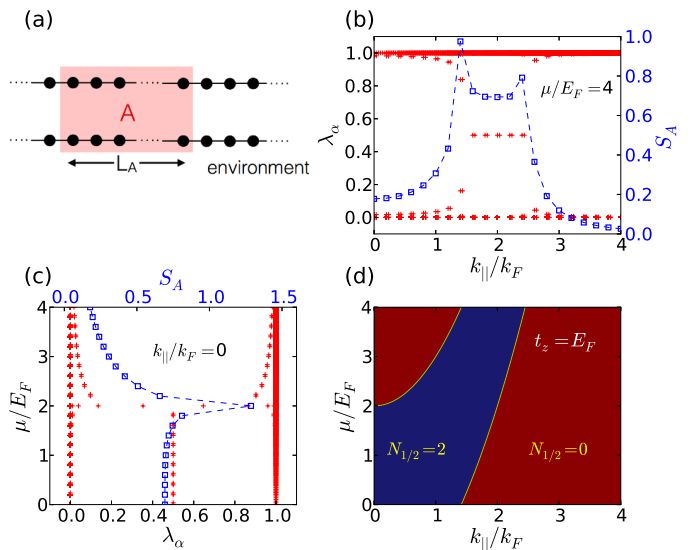


FIG. 2: (a) The whole system is divided into finite subsystem A with L_A sites and environment. Here we consider $L \gg L_A \gg 1$. (b) and (c) show the entanglement spectrum, λ_{α} , and the entanglement entropy, S_A , by choosing $t_z = E_F$ as the function of μ/E_F and k_{\parallel}/k_F respectively. (d) Phase diagram of Eq. (2) with $t_z = E_F$. $N_{1/2}$ is the number of the degenerate entanglement spectrum at $\lambda_{\alpha} = 1/2$ in the subsystem A , also indicating the number of MZM pairs at the edge.

after tracing out the environment. In our case, we numerically diagonalize the block’s Green’s function for subsystem A with a finite size, e.g., $L_A = 100$, of the ladder as shown in Fig. 2(a). The numerical results converges and is independent of the choices of subsystem in the thermal dynamic limit, $L \gg L_A \gg 1$.

In Fig. 2(b)-(c), we show the entanglement spectra λ_{α} and entanglement entropy S_A obtained by calculating the Green’s function from the effective Hamiltonian, Eq. (2). We find that the ground state becomes topologically non-trivial ($\lambda_{\alpha} = 1/2$) at exactly the same regime as Eq. (5). The entanglement entropy becomes divergent when cross the boundary. These numerical results agree with the analytic calculation of the winding number, confirming the topological properties in our current system.

Critical Temperature and Momentum Distribution: Since the topological properties are driven by the p -wave pairing in the bulk, it is also important to investigate the parameter regime for having such topological order. Different from 1D Kitaev model, the superfluidity in our current system appears in a 3D space, where the mean-field approximation is fully justified. Therefore, we can use the standard BCS theory to obtain the 3D gap function $\tilde{\Delta}_{\mathbf{q}}$ (we set $\hbar = k_B = 1$)

$$\tilde{\Delta}_{\mathbf{q}} = - \int \frac{d\mathbf{k}_{\parallel}}{(2\pi)^2} \int_{-\pi/d}^{\pi/d} \frac{dk_z}{2\pi} V_{\mathbf{k}-\mathbf{q}} \frac{\tilde{\Delta}_{\mathbf{k}}}{2E_{\mathbf{k}}} \tanh \left(\frac{E_{\mathbf{k}}}{2T} \right) \quad (6)$$

where $E_{\mathbf{q}} \equiv \sqrt{\xi_{\mathbf{q}}^2 + |\tilde{\Delta}_{\mathbf{q}}|^2}$ is Bogoliubov energy disper-

sion. Since we just consider the nearest neighboring inter-layer interaction for simplicity, the inter-layer matrix element is: $V_{\mathbf{k}} = -2\pi D^2 \cos(k_z d) |\mathbf{k}_{\parallel}| e^{-|\mathbf{k}_{\parallel}|d}$ in the limit of zero layer width, where D is the electric dipole moment [56]. The associate number equation (to determine chemical potential self-consistently) is given by

$$n_{\mathbf{k}} = \frac{1}{2} \left[1 - \frac{\xi_{\mathbf{k}}}{E_{\mathbf{k}}} \tanh \left(\frac{E_{\mathbf{k}}}{2T} \right) \right]. \quad (7)$$

We then numerical evaluate the gap function for a given temperature, and the chemical potential is determined by fixing the total particle number, $N = \sum_{\mathbf{k}} n_{\mathbf{k}}$. In Fig. 3(a) and (b), we show the density distribution in the momentum space at zero-temperature ($T = 0$). At the point(s) where the gap is closed ($k_z = 0, \pm\pi/d$), we can see $n_{\mathbf{k}} = (1 - \xi_{\mathbf{k}}/|\xi_{\mathbf{k}}|)/2$ has a discontinuous jump when $\xi_{\mathbf{k}}$ changes its sign. More precisely, the number density jumps from unity to zero at two places: (1) at $k_z = 0$ and $|\mathbf{k}_{\parallel}| = k_{Max} \equiv \sqrt{2m(\mu + 2t_z)}$, and (2) at $k_z = \pm\pi/d$ and $|\mathbf{k}_{\parallel}| = k_{Min} \equiv \sqrt{2m(\mu - 2t_z)}$ (see Fig.3(a) and (b)). We could analytically show that (see Supplemental Material) the topological order does appears exactly when the in-plane momentum is in the region between k_{Min} and k_{Max} (see Eq. (5)). As $2t_z > \mu$, the discontinuity of $n_{\mathbf{k}}$ appears only at $(|\mathbf{k}_{\parallel}|, k_z) = (k_{Max}, 0)$, showing that all the ladders are topological and MZMs covers the whole quantum number in the surface layers. In Fig. 3(c) we also show the gap function and how the critical temperature changes as t_z changes in (d). One can find that T_c has a significant drop as $t_z > \mu/2$ since the phase space for Cooper pairing shrinks. Our results show that the topological order is better observed (with a higher critical temperature) in the limit of small t_z or higher density.

Experimental Related Issues: For realistic experimental parameters, we may consider non-reactive polar molecules, $^{23}\text{Na}^{40}\text{K}$ [23] with a maximum electric dipole moment 2.7 Debye, as an example, We can load them into a 1D optical lattice with an interlayer distance $d \sim 0.25 \mu\text{m}$ with an in-plane density $n \sim 10^9 \text{ cm}^{-2}$. We then have $k_F d \sim 2.8$ and Fermi energy $E_F \sim 477 \text{ nK}$, where the critical temperature $T_c \sim 41 \text{ nK}$ as $t_z < \mu/2$ (the dipole moment is partially polarized to be $D = 0.81$ Debye). All these parameters are within current experimental conditions, showing that the p -wave superfluidity as well as the MZMs should be experimentally realizable.

When a harmonic trapping potential is included, the MZMs still exist due to the time-reversal symmetry as discussed above. We can estimate the parameter regime by applying the local density approximation, i.e. the condition for a TO becomes $|\mu - m\omega^2 \mathbf{r}_{\parallel}^2/2 - \mathbf{k}_{\parallel}^2/2m| < 2t_z$, where ω is the tapping frequency. As a result, After integrating the phase space (see Supplementary Materials), the ratio of unpaired MFs to the number of fermions in the top or bottom layer is $\eta_{\text{trap}} = \frac{4t_z\mu - 2t_z^2}{\mu^2 + 2t_z^2}$ for $2t_z < \mu$ and $\eta_{\text{trap}} = 1$ for $2t_z > \mu$. Furthermore, above condition suggest that MFs of certain in-plane kinetic energy (say, $\mathbf{k}_{\parallel}^2/2m = \mu$) have to be from certain positions,

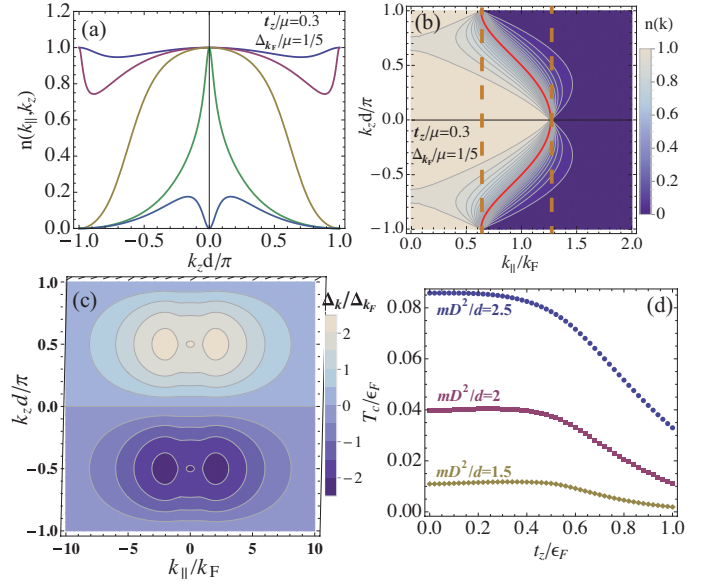


FIG. 3: (a) Momentum distribution, $n_{\mathbf{k}}$, as a function of $k_z d/\pi$ at $t_z/\mu = 0.3$. The curves from top to bottom represents $k_{\parallel}/k_F = 0, 0.6, 0.9, 1.25$ and 1.3 , respectively. (b) The contour plot of $n_{\mathbf{k}}$ at $t_z/\mu = 0.3$. The two orange dashed lines indicates k_{Max} and k_{Min} , in-between the quantum degenerate MZMs appear at the surface layers and hence a short-period interference pattern should be observed (see the text). (c) The contour plot of a typical $\tilde{\Delta}_{\mathbf{k}}$ at $k_F d = 0.5$. (d) The critical temperature T_c as function of t_z/μ at $k_F d = 2.8$. for various dipole moment strength.

$|\mathbf{r}| < 2\sqrt{t_z/m\omega^2}$. This information should help the experimental identification of these MZMs.

For experimental measurement, there has been many proposals to measure MZMs (see for example,[57]). The simplest way is by observing the long-distance correlation between MFs in the two ending layers, which should have a much shorter period in the momentum space (i.e. long time approximation of the time-of-flight experiments), $\propto \cos(k_z Ld)$. Here Ld is the distance between the top and bottom layers. Besides, the regime to find such interference pattern, $k_{Min} < |\mathbf{k}_{\parallel}| < k_{Max}$ (see Fig. 3(b)), depends on inter-layer tunneling amplitude. We emphasize that such measurement for 1D model suffers a serious noise-to-signal ratio [57], since only “one” mode at each end. In our multi-layer system, MZMs are macroscopically degenerate and makes the measurement much more promising. Finally, one can also use spatial dependent RF spectroscopy to measure the localized MFs, as discussed in Ref. [57].

Finally, we emphasize that fermionic SPT phases are not totally understood yet in 3D space, although it is argued that there exists a bulk SPT and surface symmetry enriched TO anomaly matching in a 3D bosonic weak SPT phase [3]. Furthermore, Fidkowski and Kitaev have shown [58, 59] that the non-interacting BDI class with \mathbb{Z} topological invariance shall be broken to \mathbb{Z}_8 when a short ranged four-point interaction is included. Similar

behaviors may be also appear in our system, but the classification of 3D fermionic SPT is beyond the scope of this paper. It can still be a very interesting subject for future study.

Conclusion: We propose that a novel topological state can be prepared and observed in a stack of 2D layers with fermionic polar molecules polarized to the normal direction. The associated quantum degenerate MZMs appear in the surface layers due to the 3D p -wave superfluidity,

confirmed by the winding number, entanglement spectrum and entanglement entropy numerics. We also show the parameter regime to find MZMs in the current experiments. Our work paves the way for future investigation of the many-body physics with non-Abelian statistics under time-reversal symmetry.

We thank C.-Y. Mou, S.-J. Huang, Y.-P. Huang, J.-S. You and G. Juzeliunas for valuable discussion.

-
- [1] E. Majorana, *Nuovo Cimento* **5**, 171 (1937)
- [2] C.K. Chiu, J.C.Y. Teo, A.P. Schnyder, S. Ryu - *Rev. Mod. Phys.* **88**, 035005, - APS (2016)
- [3] M. Cheng, M.Zaletel, M. Barkeshli, A.Vishwanath, and P. Bonderson *Phys. Rev. X* **6**, 041068 (2016)
- [4] A. Kitaev, *Phys. Usp.* **44** (Suppl.) (2001) 131.
- [5] L. Fu and C. L. Kane, *Phys. Rev. Lett.* **100**, 096407 (2008).
- [6] J. D. Sau, R. M. Lutchyn, S. Tewari, and S. Das Sarma, *Phys. Rev. Lett.* **104**, 040502 (2010).
- [7] J. Alicea, *Phys. Rev. B* **81**, 125318 (2010).
- [8] M. Sato, Y. Takahashi, and S. Fujimoto, *Phys. Rev. B* **82**, 134521 (2010).
- [9] R. M. Lutchyn, J. D. Sau, and S. Das Sarma, *Phys. Rev. Lett.* **105**, 077001 (2010).
- [10] V. Mourik, K. Zuo, S. M. Frolov, S. R. Plissard, E. P. A. M. Bakkers, and L. P. Kouwenhoven, *Science* **336**, 1003 (2012).
- [11] A. Das, Y. Ronen, Y. Most, Y. Oreg, M. Heiblum, and H. Shtrikman, *Nat. Phys.* **8**, 887 (2012).
- [12] L. P. Rokhinson, X. Liu, and J. K. Furdyna, *Nat. Phys.* **8**, 795 (2012).
- [13] M. T. Deng, C. L. Yu, G. Y. Huang, M. Larsson, P. Caroff, and H. Q. Xu, *Nano Lett.* **12**, 6414 (2012).
- [14] Sumanta Tewari, S. Das Sarma, Chetan Nayak, Chuanwei Zhang, and P. Zoller *Phys. Rev. Lett.* **98**, 010506 (2007)
- [15] Liang Jiang, Takuya Kitagawa, Jason Alicea, A. R. Akhmerov, David Pekker, Gil Refael, J. Ignacio Cirac, Eugene Demler, Mikhail D. Lukin, and Peter Zoller *Phys. Rev. Lett.* **106**, (2011)
- [16] Xiong-Jun Liu, K. T. Law, and T. K. Ng *Phys. Rev. Lett.* **112**, 086401 (2014);
- [17] Masatoshi Sato, Yoshiro Takahashi, and Satoshi Fujimoto *Phys. Rev. Lett.* **103**, 020401 (2009)
- [18] R. Wakatsuki, M. Ezawa, and N. Nagaosa *Phys. Rev. B* **89**, 174514 (2014)
- [19] R. Wakatsuki, M. Ezawa, Y. Tanaka, and N. Nagaosa *Phys. Rev. B* **90**, 014505 (2014)
- [20] Antonio Alecce and Luca Dell'Anna *Phys. Rev. B* **95**, 195160 (2017)
- [21] D. Vodola, L. Lepori, E. Ercolessi, A. V. Gorshkov, and G. Pupillo *Phys. Rev. Lett.* **113**, 156402 (2014)
- [22] K.-K. Ni, S. Ospelkaus, M. H. G. de Miranda, A. Peér, B. Neyenhuis, J. J. Zirbel, S. Kotochigova, P. S. Julienne, D. S. Jin, and J. Ye, *Science* **322**, 231 (2008).
- [23] C.-H. Wu, J. W. Park, P. Ahmadi, S. Will, and M. W. Zwierlein, *Phys. Rev. Lett.* **109**, 085301 (2012); J. W. Park, S. A. Will and Martin W. Zwierlein, *Phys. Rev. Lett.* **114**, 205302 (2015).
- [24] M.-S. Heo, T. T. Wang, C. A. Christensen, T. M. Rva-chov, D. A. Cotta, J.-H. Choi, Y.-R. Lee, and W. Ketterle, *Phys. Rev. A* **86**, 021602(R)(2012).
- [25] J. Deiglmayr, A. Grochola, M. Repp, K. Mrtlbauer, C. Glck, J. Lange, O. Dulieu, R. Wester and M. Weidemüller *Phys. Rev. Lett.* **101**, 133004 (2008); M. Repp, R. Pires, J. Ulmanis, R. Heck, E. D. Kuhnle, M. Weidemüller, and E. Tiemann *Phys. Rev. A* **87**, 010701(R) (2013).
- [26] B. Naylor, A. Reigue, E. Maréchal, O. Gorceix, B. Laburthe-Tolra, and L. Vernac *Phys. Rev. A* **91**, 011603(R) (2015).
- [27] M. Lu, N. Q. Burdick and B. L. Lev, *Phys. Rev. Lett.* **108**, 215301 (2012).
- [28] K. Aikawa, A. Frisch, M. Mark, S. Baier, R. Grimm, and F. Ferlaino *Phys. Rev. Lett.* **112**, 010404 (2014).
- [29] G. Quémener and J. L. Bohn, *Phys. Rev. A* **81**, 060701(2010).
- [30] A. Micheli, Z. Idziaszek, G. Pupillo, M. A. Baranov, P. Zoller, and P. S. Julienne, *Phys. Rev. Lett.* **105**, 073202(2010)
- [31] M. H. G. de Miranda, A. Chotia, B. Neyenhuis, D. Wang, G. Quemener, S. Ospelkaus, J.L. Bohn, J. Ye, and D.S. Jin, *Nature Phys.* **7**, 502 (2011).
- [32] G. M. Bruun and E. Taylor, *Phys. Rev. Lett.* **101**, 245301 (2008).
- [33] N.R. Cooper and G.V. Shlyapnikov, *Phys. Rev. Lett.* **103**, 155302 (2009).
- [34] J. Levinsen, N. R. Cooper, and G. V. Shlyapnikov, *Phys. Rev. A* **84**, 013603 (2011).
- [35] K. Sun, C. Wu, and S. Das Sarma, *Phys. Rev. B* **82**, 075105 (2010).
- [36] Y. Yamaguchi, T. Sogo, T. Ito, and T. Miyakawa, *Phys. Rev. A* **82**, 013643 (2010).
- [37] C.-K. Chan, C. Wu, W.-C. Lee, and S. Das Sarma, *Phys. Rev. A* **81**, 023602 (2010).
- [38] L. M. Sieberer and M. A. Baranov, *Phys. Rev. A* **84**, 063633 (2011).
- [39] M.M. Parish and F.M. Marchetti, *Phys. Rev. Lett.* **108**, 145304 (2012).
- [40] Z.-K. Lu and G.V. Shlyapnikov, *Phys. Rev. A* **85**, 023614 (2012).
- [41] Z.-K. Lu, S.I. Matveenko, and G. V. Shlyapnikov *Phys. Rev. A* **88**, 033625 (2013)
- [42] N. Matveeva and S. Giorgini, *Phys. Rev. Lett.* **109**, 200401 (2012).
- [43] A. Pikovski, M. Klawunn, G.V. Shlyapnikov, and L. Santos, *Phys. Rev. Lett.* **105**, 215302 (2010).
- [44] N. T. Zinner, B. Wunsch, D. Pekker, and D.-W. Wang,

- Phys. Rev. A **85**, 013603 (2012).
- [45] M. Babadi and E. Demler, Phys. Rev. B **84**, 235124 (2011).
- [46] M.A. Baranov, A. Micheli, S. Ronen, and P. Zoller, Phys. Rev. A **83**, 043602 (2011).
- [47] Fabio Cinti, Daw-Wei Wang, Massimo Boninsegni, Phys. Rev. A **95**, 023622 (2017).
- [48] A.C. Potter, E. Berg, D.-W. Wang, B.I. Halperin, and E. Demler, Phys. Rev. Lett. **105**, 220406 (2010).
- [49] S. Ospelkaus, K.-K. Ni, G. Qumner, B. Neyenhuis, D. Wang, M.H.G. de Miranda, J.L. Bohn, J. Ye, and D.S. Jin, Phys. Rev. Lett. **104**, 030402 (2010).
- [50] R. M. Lutchyn, E. Rossi, and S. Das Sarma, Phys. Rev. A **82**, 061604(R) (2010).
- [51] A. Kitaev and J. Preskill, Phys. Rev. Lett. **96** 110404 (2006). M. Levin and X. G. Wen, Phys. Rev. Lett. **96** 110405 (2006).
- [52] H. Li and F. D. M. Haldane, Phys. Rev. Lett. **101**, 010504 (2008).
- [53] F. Pollmann, E. Berg, A. M. Turner, and M. Oshikawa, Phys. Rev. B **81**, 064439 (2010). A. M. Turner, F. Pollmann and E. Berg, Phys. Rev. B **7** 075102 (2012).
- [54] S. Ryu and Y. Hatsugai, Phys. Rev. B **73** 245115 (2006).
- [55] M.-C. Chung , Y.-H. Jhu , P. Chen and S. Yip, Europhys. Lett. **95** 27003 (2011). M.-C. Chung , Y.-H. Jhu , P. Chen and C.-Y. Mou, Journal of Physics: Condensed Matter **25** 28 (2013).
- [56] H. Lee, S. I. Matveenko, D.-W. Wang and G. V. Shlyapnikov, arXiv:1705.06637 (2017).
- [57] C.V. Kraus, S. Diehl, P. Zoller, and M.A. Baranov, New J. Phys. **14** 113036 (2012).
- [58] L. Fidkowski and A. Kitaev Phys. Rev. B **83**, 075103 (2011)
- [59] L. Fidkowski and A. Kitaev Phys. Rev. B **81**, 134509 (2010)

Supplemental Material for Quantum Degenerate Majorana Zero Modes in Two-Dimensional continuous Space

Yen-Ting Lin¹, Ching-Yu Huang², Hao Lee¹, Daw-Wei Wang^{1,2}

¹ *Physics Department, National Tsing Hua University, Hsinchu, Taiwan*

² *Physics Division, National Center for Theoretical Sciences, Hsinchu, Taiwan*

(Dated: December 14, 2024)

In the Supplemental Material, we first show how the unpaired Majorana fermions (MFs) can be analytically obtained from the Bogoliubov-de Gennes's equation in section A. In section B, we show why the MZMs obtained in this paper is stable against any single particle perturbation under time-reversal symmetry. In section C we explicitly show the condition for BDI class and the calculation of winding number. In section D, we show how to estimate the number of unpaired MFs both in a translationally invariant 2D layer system and in a finite size system with a harmonic trapping potential within the local density approximation. Finally, we find the connection between \mathbb{Z}_2 index and the number equation shown in section E.

A: WAVEFUNCTIONS OF UNPAIRED MAJORANA FERMIONS IN A KITAEV'S LADDER FOR $\mu - \mathbf{k}_{\parallel}^2/2m = 0$ AND $\Delta_{\mathbf{k}_{\parallel}} = t_z$

To see how MFs appears in $H_{\mathbf{k}_{\parallel}}^{\text{ladd}}$, we first note that the definition of Majorana fermions (MFs) in real space is different from that in momentum space. For a general fermionic field operator $C(x)$ in position x , its relation with MF operator, $\Gamma(x)$, are following:

$$\begin{aligned} C(x) &= \frac{1}{2} \left(\Gamma_1(x) + i \Gamma_2(x) \right) \\ C^\dagger(x) &= \frac{1}{2} \left(\Gamma_1(x) - i \Gamma_2(x) \right), \end{aligned} \quad (1)$$

and

$$\begin{aligned} \Gamma_1(x) &= C(x) + C^\dagger(x) \\ \Gamma_2(x) &= -i \left(C(x) - C^\dagger(x) \right). \end{aligned} \quad (2)$$

Therefore, by doing Fourier Transformation, the Majorana operators in momentum space can be given

$$\begin{aligned} \Gamma_{1,k} &= \int \Gamma_1(x) e^{-ikx} dx = \int C(x) e^{-ikx} dx + \int C^\dagger(x) e^{-ikx} dx \\ &= C_k + C_{-k}^\dagger, \\ \Gamma_{2,k} &= -i \left(C_k - C_{-k}^\dagger \right). \end{aligned} \quad (3)$$

We note that now the MF operator $\Gamma_{1/2,k}$ are composed by Dirac fermionic operator and its anti-particles in the momentum k and $-k$ respectively. This indicates that the two Kitaev's ladder in our systems are originally from the same representation of MF operators.

Therefore, now using similar notation, we can define MFs in our present case as following:

$$\begin{aligned} c_{\mathbf{k}_{\parallel},j} &= \frac{1}{2} \left[\gamma_{\mathbf{k}_{\parallel},j}^{(1)} + i \gamma_{\mathbf{k}_{\parallel},j}^{(2)} \right], \\ c_{\mathbf{k}_{\parallel},j}^\dagger &= \frac{1}{2} \left[\gamma_{-\mathbf{k}_{\parallel},j}^{(1)} - i \gamma_{-\mathbf{k}_{\parallel},j}^{(2)} \right], \\ c_{-\mathbf{k}_{\parallel},j} &= \frac{1}{2} \left[\gamma_{-\mathbf{k}_{\parallel},j}^{(1)} + i \gamma_{-\mathbf{k}_{\parallel},j}^{(2)} \right], \\ c_{-\mathbf{k}_{\parallel},j}^\dagger &= \frac{1}{2} \left[\gamma_{\mathbf{k}_{\parallel},j}^{(1)} - i \gamma_{\mathbf{k}_{\parallel},j}^{(2)} \right] \end{aligned} \quad (4)$$

Since we are considering a special case: $\Delta_{\mathbf{k}_{\parallel}} = t_z$, and the Kitaev's ladder Hamiltonian can then be written as

$$H_{\mathbf{k}_{\parallel}}^{\text{ladd}} = -t_z \sum_{j=1}^{L-1} \left[c_{\mathbf{k}_{\parallel},j}^{\dagger} c_{\mathbf{k}_{\parallel},j+1} + c_{-\mathbf{k}_{\parallel},j}^{\dagger} c_{-\mathbf{k}_{\parallel},j+1} + c_{\mathbf{k}_{\parallel},j}^{\dagger} c_{-\mathbf{k}_{\parallel},j+1}^{\dagger} + c_{-\mathbf{k}_{\parallel},j}^{\dagger} c_{\mathbf{k}_{\parallel},j+1}^{\dagger} + c_{\mathbf{k}_{\parallel},j+1}^{\dagger} c_{\mathbf{k}_{\parallel},j} + c_{-\mathbf{k}_{\parallel},j+1}^{\dagger} c_{-\mathbf{k}_{\parallel},j} + c_{-\mathbf{k}_{\parallel},j+1}^{\dagger} c_{\mathbf{k}_{\parallel},j} + c_{\mathbf{k}_{\parallel},j+1}^{\dagger} c_{-\mathbf{k}_{\parallel},j} \right] \quad (5)$$

where L is the number site of z-direction.

After some straightforward algebra, the first four terms in [] of Hamiltonian is given by

$$\begin{aligned} & \frac{1}{4}(\gamma_{-\mathbf{k}_{\parallel},j}^{(1)} - i\gamma_{-\mathbf{k}_{\parallel},j}^{(2)})(\gamma_{\mathbf{k}_{\parallel},j+1}^{(1)} + i\gamma_{\mathbf{k}_{\parallel},j+1}^{(2)}) + \\ & \frac{1}{4}(\gamma_{\mathbf{k}_{\parallel},j}^{(1)} - i\gamma_{\mathbf{k}_{\parallel},j}^{(2)})(\gamma_{-\mathbf{k}_{\parallel},j+1}^{(1)} + i\gamma_{-\mathbf{k}_{\parallel},j+1}^{(2)}) + \\ & \frac{1}{4}(\gamma_{-\mathbf{k}_{\parallel},j}^{(1)} - i\gamma_{-\mathbf{k}_{\parallel},j}^{(2)})(\gamma_{\mathbf{k}_{\parallel},j+1}^{(1)} - i\gamma_{\mathbf{k}_{\parallel},j+1}^{(2)}) + \\ & \frac{1}{4}(\gamma_{\mathbf{k}_{\parallel},j}^{(1)} - i\gamma_{\mathbf{k}_{\parallel},j}^{(2)})(\gamma_{-\mathbf{k}_{\parallel},j+1}^{(1)} - i\gamma_{-\mathbf{k}_{\parallel},j+1}^{(2)}) \\ & = \frac{1}{4}(\gamma_{-\mathbf{k}_{\parallel},j}^{(1)}\gamma_{\mathbf{k}_{\parallel},j+1}^{(1)} + \gamma_{-\mathbf{k}_{\parallel},j}^{(2)}\gamma_{\mathbf{k}_{\parallel},j+1}^{(2)}) + \frac{i}{4}(\gamma_{-\mathbf{k}_{\parallel},j}^{(1)}\gamma_{\mathbf{k}_{\parallel},j+1}^{(2)} - \gamma_{-\mathbf{k}_{\parallel},j}^{(2)}\gamma_{\mathbf{k}_{\parallel},j+1}^{(1)}) + \\ & \frac{1}{4}(\gamma_{\mathbf{k}_{\parallel},j}^{(1)}\gamma_{-\mathbf{k}_{\parallel},j+1}^{(1)} + \gamma_{\mathbf{k}_{\parallel},j}^{(2)}\gamma_{-\mathbf{k}_{\parallel},j+1}^{(2)}) + \frac{i}{4}(\gamma_{\mathbf{k}_{\parallel},j}^{(1)}\gamma_{-\mathbf{k}_{\parallel},j+1}^{(2)} - \gamma_{\mathbf{k}_{\parallel},j}^{(2)}\gamma_{-\mathbf{k}_{\parallel},j+1}^{(1)}) + \\ & \frac{1}{4}(\gamma_{-\mathbf{k}_{\parallel},j}^{(1)}\gamma_{\mathbf{k}_{\parallel},j+1}^{(1)} - \gamma_{-\mathbf{k}_{\parallel},j}^{(2)}\gamma_{\mathbf{k}_{\parallel},j+1}^{(2)}) + \frac{-i}{4}(\gamma_{-\mathbf{k}_{\parallel},j}^{(1)}\gamma_{\mathbf{k}_{\parallel},j+1}^{(2)} + \gamma_{-\mathbf{k}_{\parallel},j}^{(2)}\gamma_{\mathbf{k}_{\parallel},j+1}^{(1)}) + \\ & \frac{1}{4}(\gamma_{\mathbf{k}_{\parallel},j}^{(1)}\gamma_{-\mathbf{k}_{\parallel},j+1}^{(1)} - \gamma_{\mathbf{k}_{\parallel},j}^{(2)}\gamma_{-\mathbf{k}_{\parallel},j+1}^{(2)}) + \frac{-i}{4}(\gamma_{\mathbf{k}_{\parallel},j}^{(1)}\gamma_{-\mathbf{k}_{\parallel},j+1}^{(2)} + \gamma_{\mathbf{k}_{\parallel},j}^{(2)}\gamma_{-\mathbf{k}_{\parallel},j+1}^{(1)}) \end{aligned} \quad (6)$$

Similarly, the last four terms in [] is given by

$$\begin{aligned} & \frac{1}{4}(\gamma_{-\mathbf{k}_{\parallel},j+1}^{(1)} - i\gamma_{-\mathbf{k}_{\parallel},j+1}^{(2)})(\gamma_{\mathbf{k}_{\parallel},j}^{(1)} + i\gamma_{\mathbf{k}_{\parallel},j}^{(2)}) + \\ & \frac{1}{4}(\gamma_{\mathbf{k}_{\parallel},j+1}^{(1)} - i\gamma_{\mathbf{k}_{\parallel},j+1}^{(2)})(\gamma_{-\mathbf{k}_{\parallel},j}^{(1)} + i\gamma_{-\mathbf{k}_{\parallel},j}^{(2)}) + \\ & \frac{1}{4}(\gamma_{-\mathbf{k}_{\parallel},j+1}^{(1)} + i\gamma_{-\mathbf{k}_{\parallel},j+1}^{(2)})(\gamma_{\mathbf{k}_{\parallel},j}^{(1)} + i\gamma_{\mathbf{k}_{\parallel},j}^{(2)}) + \\ & \frac{1}{4}(\gamma_{\mathbf{k}_{\parallel},j+1}^{(1)} + i\gamma_{\mathbf{k}_{\parallel},j+1}^{(2)})(\gamma_{-\mathbf{k}_{\parallel},j}^{(1)} + i\gamma_{-\mathbf{k}_{\parallel},j}^{(2)}) \\ & = \frac{1}{4}(\gamma_{-\mathbf{k}_{\parallel},j+1}^{(1)}\gamma_{\mathbf{k}_{\parallel},j}^{(1)} + \gamma_{-\mathbf{k}_{\parallel},j+1}^{(2)}\gamma_{\mathbf{k}_{\parallel},j}^{(2)}) + \frac{i}{4}(\gamma_{-\mathbf{k}_{\parallel},j+1}^{(1)}\gamma_{\mathbf{k}_{\parallel},j}^{(2)} - \gamma_{-\mathbf{k}_{\parallel},j+1}^{(2)}\gamma_{\mathbf{k}_{\parallel},j}^{(1)}) + \\ & \frac{1}{4}(\gamma_{\mathbf{k}_{\parallel},j+1}^{(1)}\gamma_{-\mathbf{k}_{\parallel},j}^{(1)} + \gamma_{\mathbf{k}_{\parallel},j+1}^{(2)}\gamma_{-\mathbf{k}_{\parallel},j}^{(2)}) + \frac{i}{4}(\gamma_{\mathbf{k}_{\parallel},j+1}^{(1)}\gamma_{-\mathbf{k}_{\parallel},j}^{(2)} - \gamma_{\mathbf{k}_{\parallel},j+1}^{(2)}\gamma_{-\mathbf{k}_{\parallel},j}^{(1)}) + \\ & \frac{1}{4}(\gamma_{-\mathbf{k}_{\parallel},j+1}^{(1)}\gamma_{\mathbf{k}_{\parallel},j}^{(1)} - \gamma_{-\mathbf{k}_{\parallel},j+1}^{(2)}\gamma_{\mathbf{k}_{\parallel},j}^{(2)}) + \frac{i}{4}(\gamma_{-\mathbf{k}_{\parallel},j+1}^{(1)}\gamma_{\mathbf{k}_{\parallel},j}^{(2)} + \gamma_{-\mathbf{k}_{\parallel},j+1}^{(2)}\gamma_{\mathbf{k}_{\parallel},j}^{(1)}) + \\ & \frac{1}{4}(\gamma_{\mathbf{k}_{\parallel},j+1}^{(1)}\gamma_{-\mathbf{k}_{\parallel},j}^{(1)} - \gamma_{\mathbf{k}_{\parallel},j+1}^{(2)}\gamma_{-\mathbf{k}_{\parallel},j}^{(2)}) + \frac{i}{4}(\gamma_{\mathbf{k}_{\parallel},j+1}^{(1)}\gamma_{-\mathbf{k}_{\parallel},j}^{(2)} + \gamma_{\mathbf{k}_{\parallel},j+1}^{(2)}\gamma_{-\mathbf{k}_{\parallel},j}^{(1)}) \end{aligned} \quad (7)$$

Now using the the anti-commutation relations, $\{\gamma_{j,\mathbf{k}}^{(a)}, \gamma_{j',\mathbf{k}'}^{(b)}\} = 2\delta_{j,j'}\delta_{a,b}\delta_{\mathbf{k},\mathbf{k}'}$ ($a, b = 1, 2$), we can obtain the Hamiltonian with special case $\Delta_{\mathbf{k}_{\parallel}} = t_z$,

$$H_{\mathbf{k}_{\parallel}}^{\text{ladd}} = it_z \sum_{j=1}^{L-1} \left(\gamma_{\mathbf{k}_{\parallel},j}^{(2)}\gamma_{-\mathbf{k}_{\parallel},j+1}^{(1)} + \gamma_{-\mathbf{k}_{\parallel},j}^{(2)}\gamma_{\mathbf{k}_{\parallel},j+1}^{(1)} \right). \quad (8)$$

We note that the above Hamiltonian can be mapped to to Dirac fermion by defining $a_{\mathbf{k}_{\parallel},j} \equiv \gamma_{\mathbf{k}_{\parallel},j+1}^{(1)} + i\gamma_{\mathbf{k}_{\parallel},j}^{(2)}$, $a_{\mathbf{k}_{\parallel},j}^{\dagger} \equiv \gamma_{-\mathbf{k}_{\parallel},j+1}^{(1)} - i\gamma_{-\mathbf{k}_{\parallel},j}^{(2)}$:

$$H_{\mathbf{k}_{\parallel}}^{\text{ladd}} = \frac{-t_z}{2} \sum_{j=1}^{L-1} \left(a_{\mathbf{k}_{\parallel},j}^{\dagger} a_{\mathbf{k}_{\parallel},j} + a_{-\mathbf{k}_{\parallel},j}^{\dagger} a_{-\mathbf{k}_{\parallel},j} \right). \quad (9)$$

Therefore, it is easy to see that we missed unpaired MFs $\gamma_{\pm\mathbf{k}_{\parallel},1}^{(1)}$ in the bottom layer ($j = 1$) and $\gamma_{\pm\mathbf{k}_{\parallel},L}^{(2)}$ in the top layer ($j = L$).

B: STABILITY OF TOPOLOGICAL ORDER UNDER TIME-REVERSAL SYMMETRY

In this session we show that the unpaired MFs (i.e. MZMs) obtained from the Kitaev ladder are stable against recombination due to a general perturbation under time-reversal symmetry (TRS) and in-plane parity symmetry (PS). As described in main text, the quantum degenerate MZMs are distributed in the momentum range, R , where $k_{Min} < |\mathbf{k}_{\parallel}| < k_{Max}$. Here $k_{Max} = \sqrt{2m(\mu + 2t_z)}$ and $k_{Min} = \sqrt{2m(\mu - 2t_z)}$ for $\mu > t_z$ or 0 otherwise.

As a result, the most general single particle perturbation on these unpaired MFs in the bottom layer ($j = 1$) is of the following form:

$$H_1 = i \sum_{\mathbf{k}, \mathbf{k}' \in R} A(\mathbf{k}_{\parallel}, \mathbf{k}'_{\parallel}) \tilde{\gamma}_{\mathbf{k}_{\parallel},1}^{(1)} \tilde{\gamma}_{\mathbf{k}'_{\parallel},1}^{(1)} \quad (10)$$

where we have redefined that all the unpaired MFs to be $\tilde{\gamma}_{\mathbf{k}_{\parallel},1}^{(1)}$ (when $\mu - \mathbf{k}_{\parallel}^2/2m \neq 0$ or $t_z \neq \Delta_{\mathbf{k}_{\parallel}}$, we just need to have some linear combination of original MFs), which satisfies the following statistics: $\{\tilde{\gamma}_{\mathbf{k}_{\parallel},1}^{(1)}, \tilde{\gamma}_{\mathbf{k}'_{\parallel},1}^{(1)}\} = 2\delta_{\mathbf{k}_{\parallel}, \mathbf{k}'_{\parallel}}$, and has the same eigenvalue for time-reversal operation: $\mathcal{T}\tilde{\gamma}_{\mathbf{k}_{\parallel},1}^{(1)}\mathcal{T}^{-1} = \tilde{\gamma}_{-\mathbf{k}_{\parallel},1}^{(1)}$. As a result, the function $A(\mathbf{k}_{\parallel}, \mathbf{k}'_{\parallel})$ has to satisfied at least the following two conditions:

(1) Hermitian of H' gives $(\tilde{\gamma}_{\mathbf{k}_{\parallel},1}^{(1)})^\dagger = \tilde{\gamma}_{-\mathbf{k}_{\parallel},1}^{(1)}$ as shown in the previous session)

$$A(\mathbf{k}_{\parallel}, \mathbf{k}'_{\parallel}) = A(-\mathbf{k}_{\parallel}, -\mathbf{k}'_{\parallel})^*, \quad (11)$$

because

$$\begin{aligned} H_1 = H_1^\dagger &= -i \sum_{\mathbf{k}, \mathbf{k}' \in R} A(\mathbf{k}_{\parallel}, \mathbf{k}'_{\parallel})^* \tilde{\gamma}_{-\mathbf{k}'_{\parallel},1}^{(1)} \tilde{\gamma}_{-\mathbf{k}_{\parallel},1}^{(1)} \\ &= i \sum_{\mathbf{k}, \mathbf{k}' \in R} A(\mathbf{k}_{\parallel}, \mathbf{k}'_{\parallel})^* \tilde{\gamma}_{-\mathbf{k}_{\parallel},1}^{(1)} \tilde{\gamma}_{-\mathbf{k}'_{\parallel},1}^{(1)} \\ &= i \sum_{\mathbf{k}, \mathbf{k}' \in R} A(-\mathbf{k}_{\parallel}, -\mathbf{k}'_{\parallel})^* \tilde{\gamma}_{\mathbf{k}_{\parallel},1}^{(1)} \tilde{\gamma}_{\mathbf{k}'_{\parallel},1}^{(1)} \end{aligned} \quad (12)$$

(2) Time-reversal symmetry gives

$$A(\mathbf{k}_{\parallel}, \mathbf{k}'_{\parallel}) = -A(-\mathbf{k}_{\parallel}, -\mathbf{k}'_{\parallel})^*, \quad (13)$$

because

$$\begin{aligned} H_1 = \mathcal{T}H_1\mathcal{T}^{-1} &= -i \sum_{\mathbf{k}, \mathbf{k}' \in R} A(\mathbf{k}_{\parallel}, \mathbf{k}'_{\parallel})^* \tilde{\gamma}_{-\mathbf{k}_{\parallel},1}^{(1)} \tilde{\gamma}_{-\mathbf{k}'_{\parallel},1}^{(1)} \\ &= -i \sum_{\mathbf{k}, \mathbf{k}' \in R} A(-\mathbf{k}_{\parallel}, -\mathbf{k}'_{\parallel})^* \tilde{\gamma}_{\mathbf{k}_{\parallel},1}^{(1)} \tilde{\gamma}_{\mathbf{k}'_{\parallel},1}^{(1)} \end{aligned} \quad (14)$$

One can see easily that the function $A(\mathbf{k}_{\parallel}, \mathbf{k}'_{\parallel}) = 0$ because Eq. (11) and Eq. (13) cannot be satisfied simultaneously unless zero. Therefore, the system composed by single type of MFs should be stable against any single particle perturbation (whether a local disorder potential or a global trapping potential) when the time-reversal symmetry is applied.

C: BDI CLASS AND WINDING NUMBER

In order to specify the TO, we have to check the symmetry first.

$$\mathcal{T}H(\mathbf{k})\mathcal{T}^{-1} = H(-\mathbf{k}), \quad (15)$$

$$\mathcal{C}H(\mathbf{k})\mathcal{C}^{-1} = -H(-\mathbf{k}), \quad (16)$$

$$\mathcal{S}H(\mathbf{k})\mathcal{S}^{-1} = -H(\mathbf{k}). \quad (17)$$

Where \mathcal{T} , \mathcal{C} , and \mathcal{S} are the anti-unitary time reversal symmetry (complex conjugate for spinless model), particle-hole symmetry and chiral symmetry (product of \mathcal{T} and \mathcal{C}). It belongs to BDI class and topological phases is characterized by the \mathbb{Z} index. This topological state is protected by chiral symmetry.

The BdG Hamiltonian can be unitary transformed to off-diagonal form, $H_{BdG} = \frac{i}{4} \sum_{\mathbf{k}} \Gamma_{\mathbf{k}}^{\dagger} \begin{bmatrix} 0 & v_{\mathbf{k}} \\ v_{\mathbf{k}}^{\dagger} & 0 \end{bmatrix} \Gamma_{\mathbf{k}}$, where $\mu_{\mathbf{k}_{\parallel}} = \mu + \frac{k_{\parallel}^2}{2m}$ and $v_{\mathbf{k}} = -\mu_{\mathbf{k}_{\parallel}} - 2t_z \cos k_z - 2i\Delta \sin k_z$. $v_{\mathbf{k}} = R(\mathbf{k})e^{i\theta(\mathbf{k})}$. Then, the corresponding Q-matrix can be given, $Q_{\mathbf{k}} = \begin{bmatrix} 0 & q_{\mathbf{k}} \\ q_{\mathbf{k}}^{\dagger} & 0 \end{bmatrix}$, where $q_{\mathbf{k}} = \frac{v_{\mathbf{k}}}{|v_{\mathbf{k}}|} = e^{i\theta_{\mathbf{k}_{\parallel}, k_z}}$. The relevant space is the U(N) unitary group. $q_{\mathbf{k}}$ is a mapping from z-direction BZ to U(N), which topologically classified by first homotopy group, $\Pi_1[U(N)] = \mathbb{Z}$, characterized by the winding number W, see Ref([1]). The winding number can be calculated as following:

$$\begin{aligned}
W_{\mathbf{k}_{\parallel}} &\equiv \int_{-\pi/d}^{\pi/d} \frac{dk_z}{2\pi} \partial_{k_z} \theta_{\mathbf{k}_{\parallel}, k_z} \\
&= \int_{-\pi/d}^{\pi/d} \frac{dk_z}{2\pi} \frac{\partial_{k_z} [-\cos \theta_{\mathbf{k}_{\parallel}, k_z}]}{\sin \theta_{\mathbf{k}_{\parallel}, k_z}} \\
&= \int_{-\pi/d}^{\pi/d} \frac{dk_z}{-2\pi} \frac{\partial_{k_z} [-(\mu_{\mathbf{k}_{\parallel}} + 2t_z \cos k_z)/R(\mathbf{k})]}{-[2\Delta_{\mathbf{k}_{\parallel}} \sin k_z]/R(\mathbf{k})} \\
&= \frac{1}{4\pi} \int_{-\pi}^{\pi} dk_z \frac{1}{\Delta_{\mathbf{k}_{\parallel}} \sin k_z} \left[2t_z \sin k_z + 2 \frac{[\mu_{\mathbf{k}_{\parallel}} + 2t_z \cos k_z]}{R(\mathbf{k})^2} [2\Delta_{\mathbf{k}_{\parallel}}^2 \sin k_z \cos k_z - t_z \sin k_z (\mu_{\mathbf{k}_{\parallel}} + 2t_z \cos k_z)] \right] \\
&= \frac{1}{2\pi \Delta_{\mathbf{k}_{\parallel}}} \int_{-\pi}^{\pi} dk_z \frac{4\Delta_{\mathbf{k}_{\parallel}}^2 t_z + 2\Delta_{\mathbf{k}_{\parallel}}^2 \mu_{\mathbf{k}_{\parallel}} \cos k_z}{[\mu_{\mathbf{k}_{\parallel}} + 2t_z \cos k_z]^2 + 4\Delta_{\mathbf{k}_{\parallel}}^2 \sin^2 k_z} \tag{18}
\end{aligned}$$

Changing the variables $z = e^{ik_z}$ and let $J_1 = \frac{t_z + \Delta_{\mathbf{k}_{\parallel}}}{\mu_{\mathbf{k}_{\parallel}}}$, $J_2 = \frac{t_z - \Delta_{\mathbf{k}_{\parallel}}}{\mu_{\mathbf{k}_{\parallel}}}$, and $J_{\pm} = J_1 \pm J_2$,

$$\begin{aligned}
W_{\mathbf{k}_{\parallel}} &= \frac{1}{2\pi i} \oint \frac{dz}{z} \Delta_{\mathbf{k}_{\parallel}} \frac{4t_z + \mu_{\mathbf{k}_{\parallel}} (z + \frac{1}{z})}{[\mu_{\mathbf{k}_{\parallel}} + t_z (z + \frac{1}{z})]^2 - \Delta_{\mathbf{k}_{\parallel}}^2 (z - \frac{1}{z})^2} \\
&= \frac{\Delta_{\mathbf{k}_{\parallel}}}{2\pi i} \oint dz \frac{\mu_{\mathbf{k}_{\parallel}} z^2 + 4t_z z + \mu_{\mathbf{k}_{\parallel}}}{[(t_z + \Delta_{\mathbf{k}_{\parallel}})z^2 + \mu_{\mathbf{k}_{\parallel}}z + (t_z - \Delta_{\mathbf{k}_{\parallel}})] [(t_z - \Delta_{\mathbf{k}_{\parallel}})z^2 + \mu_{\mathbf{k}_{\parallel}}z + (t_z + \Delta_{\mathbf{k}_{\parallel}})]} \\
&= \frac{J_-}{2} \oint \frac{dz}{2\pi i} \frac{z^2 + 2J_+ z + 1}{[J_1 z^2 + z + J_2][J_2 z^2 + z + J_1]} \\
&= \frac{J_-}{2} \oint \frac{dz}{2\pi i} \frac{z^2 + 2J_+ z + 1}{J_1 J_2 [(z - Z_1)(z - Z_2)(z - Z_3)(z - Z_4)]} \tag{19} \\
&\tag{20}
\end{aligned}$$

Four poles of the function are $Z_{1,2} = \frac{-1 \pm \sqrt{1 - 4J_1 J_2}}{2J_1}$ and $Z_{3,4} = \frac{-1 \pm \sqrt{1 - 4J_1 J_2}}{2J_2}$ respectively. It can be shown that $Z_{3,4} = 1/Z_{1,2}$. By Cauchy's residue theorem, the winding number and the phase boundary can be determined. There are three different situations:

$$A: \text{ If } |Z_1| < 1 \text{ and } |Z_2| < 1, \text{ then } W = 1. \tag{21}$$

$$B: \text{ If } |Z_3| < 1 \text{ and } |Z_4| < 1, \text{ then } W = -1. \tag{22}$$

$$C: \text{ If } |Z_1| < 1 \text{ and } |Z_3| < 1, \text{ or } |Z_2| < 1 \text{ and } |Z_4| < 1, \text{ then } W = 0. \tag{23}$$

They are three distinguish z-direction gapped phases, where A and B conditions corresponding to two different non-trivial topological phases. The corresponding Q matrix element are winding around origin of complex plane counterclockwise and clockwise respectively. Phase boundaries are determined by $|Z_{1,2}| = |Z_{3,4}| = 1$,

$$\begin{aligned}
&-1 \pm \sqrt{1 - 4J_1 J_2} = \pm 2J_1 \\
\Rightarrow &1 - 4J_1 J_2 = 1 \pm 4J_1 + 4J_1^2 \\
\Rightarrow &J_1 + J_2 = \pm 1 \\
\Rightarrow &\mu_{\mathbf{k}_{\parallel}} = \pm 2t_z
\end{aligned}$$

where consistent with the closing gap topological transition. Finally, we can solve the topological non-trivial conditions for A and B situations:

$$|\mu_{\mathbf{k}_{\parallel}}| = \left| -\mu + \frac{k_{\parallel}^2}{2m} \right| < 2t_z.$$

D: RATIO OF UNPAIRED MAJORANA FERMIONS TO THE TOTAL NUMBER OF FERMIONS IN THE EDGE LAYERS

To estimate the number of unpaired MFs in a translationally invariant 2D layer system, we first calculate the average number of states in each layer (and hence also in the top and bottom layer respectively), since it is not a fix number due to the presence of interlayer tunneling. We can first calculate the total number of states by assuming the gap function is so small compared to the Fermi energy that the Fermi sea is almost identical to the noninteracting one. As a result, the average number of states occupied in a 2D layer can be estimated as following:

$$\begin{aligned} N_{2D} &= \frac{\Omega L d}{L} \int \frac{d\mathbf{k}_{\parallel}}{(2\pi)^2} \int_{-\pi/d}^{\pi/d} \frac{dk_z}{2\pi} \theta(\mu - \mathbf{k}_{\parallel}^2/2m + 2t_z \cos(k_z d)) \\ &= \frac{m\Omega}{(2\pi)^2} \int_{-\pi}^{\pi} dy (\mu + 2t_z \cos(y)) \\ &= \frac{m\Omega\mu}{2\pi}, \end{aligned} \quad (24)$$

where Ω stands for the 2D area, and we have integrating out the in-plane degree of freedom first to have the last line. It is easy to show this result is identical to a 2D system with total chemical potential, $\mu = k_F^2/2m$, where k_F is the Fermi momentum. In other words, we can present the "effectively" 2D Fermi sphere as the one shown in Fig. 1(a).

However, not all these states support unpaired MFs, unless it satisfies the following condition (see Eq. (6) of the main text):

$$|\mu_{\mathbf{k}_{\parallel}}| = \left| \mu - \mathbf{k}_{\parallel}^2/2m \right| < 2t_z. \quad (25)$$

To calculate the total number of states, which satisfies Eq. (25), can be calculated to be (assuming $2t_z < \mu$ first)

$$\begin{aligned} N_{MF} &= \Omega \int \frac{d\mathbf{k}_{\parallel}}{(2\pi)^2} \theta(\mu - \mathbf{k}_{\parallel}^2/2m) \theta(\mathbf{k}_{\parallel}^2/2m - \mu + 2t_z) \\ &= \frac{\Omega m}{2\pi} \int_{\mu-2t_z}^{\mu} dE_K = \frac{1}{\pi} m t_z \Omega, \end{aligned} \quad (26)$$

where $E_K \equiv k_{\parallel}^2/2m$. $\theta(x) = 1$ for $x > 0$ and 0 else is the Heaviside function.

As a result, the ratio of number of MFs to the average number of states in the top or bottom layers is given by

$$\eta_{\text{plane}} = \frac{N_{MF}}{N_{2D}} = \frac{2t_z}{\mu}. \quad (27)$$

for $2t_z < \mu$. When $2t_z > \mu$, all Kitaev's ladder can support unpaired MFs and hence the occupation ratio $\eta = 1$. As a result, we have $\eta = \text{Min}(\mu, 2t_z)/\mu$ for a 2D system with in-plane translational invariance.

When considering the presence of a harmonic trapping potential in a realistic experiment, although the translational symmetry is broken, the MZMs proposed in this paper still exist due to the conservation of time-reversal symmetry. The available parameter regime for finding these MZMs may be changed due to the inhomogeneous density distribution, but can be estimated by using local density (i.e. semi-classical) approximation, i.e. $\mu(r) \equiv \mu - m\omega^2 \mathbf{r}_{\parallel}^2/2$, where ω is the tapping frequency.

Again, we first calculate the average number of states occupied in each layer from the semi-classical approximation:

$$\begin{aligned}
N_{2D} &= \frac{1}{L} \int d\mathbf{r} \int \frac{d\mathbf{k}_{\parallel}}{(2\pi)^2} \int_{-\pi/d}^{\pi/d} \frac{dk_z}{2\pi} \theta \left(\mu - \frac{\mathbf{k}_{\parallel}^2}{2m} + 2t_z \cos(k_z d) - \frac{1}{2} m\omega^2 \mathbf{r}_{\parallel}^2 \right) \\
&= \frac{m}{(2\pi)^2 m\omega^2} \int_0^{\infty} dE_R \int_0^{\infty} dE_K \int_{-\pi}^{\pi} dy \theta(\mu - E_K - E_R + 2t_z \cos(y)) \\
&= \frac{m}{(2\pi)^2 m\omega^2} \int_0^{\infty} dE_{KR} \int_{-E_{ER}/2}^{E_{KR}/2} dx \int_{-\pi}^{\pi} dy \theta(\mu - E_{KR} + 2t_z \cos(y)) \\
&= \frac{m}{(2\pi)^2 m\omega^2} \int_0^{\infty} dE_{KR} \int_{-\pi}^{\pi} dy E_{KR} \theta(\mu - E_{KR} + 2t_z \cos(y)) \\
&= \frac{m}{(2\pi)^2 m\omega^2} \int_{-\pi}^{\pi} dy \int_0^{\mu+2t_z \cos(y)} dE_{KR} E_{KR} \\
&= \frac{m}{2(2\pi)^2 m\omega^2} \int_{-\pi}^{\pi} dy (\mu + 2t_z \cos(y))^2 \\
&= \frac{1}{4\pi\omega^2} [\mu^2 + 2t_z^2]
\end{aligned} \tag{28}$$

where we have changed variables to be $E_{KR} \equiv E_K + E_R$, $x \equiv (E_K - E_R)/2$, $E_K \equiv \mathbf{k}_{\parallel}^2/2m$ and $E_R \equiv m\omega^2 \mathbf{r}_{\parallel}^2/2$. One can check Fig. 1(b) for mode details of the calculation. The obtained result is equivalent to a pure 2D system in a harmonic potential with chemical potential, $\tilde{\mu} \equiv \sqrt{\mu^2 + 2t_z^2}$.

To calculate the number of states satisfying $|\mu - m\omega^2 \mathbf{r}_{\parallel}^2/2 - \mathbf{k}_{\parallel}^2/2m| < 2t_z$, It is easy to show that it implies that $E_K + E_R = \mathbf{k}_{\parallel}^2/2m + m\omega^2 \mathbf{r}_{\parallel}^2/2$ has to be larger than $\mu - 2t_z$ but smaller than $\tilde{\mu}$. Therefore the total number of states to have unpaired MFs can be estimated to be

$$\begin{aligned}
N_{MF} &= \frac{1}{4\pi\omega^2} [\mu^2 + 2t_z^2] - \frac{1}{4\pi\omega^2} (\mu - 2t_z)^2 \\
&= \frac{t_z(\mu - t_z/2)}{\pi\omega^2}
\end{aligned} \tag{29}$$

As a result, the ratio to have unpaired MF in the top or bottom layers is

$$\eta_{\text{trap}} \equiv \frac{N_{MF}}{N_{2D}} = \frac{4t_z\mu - 2t_z^2}{\mu^2 + 2t_z^2}, \tag{30}$$

which is therefore very different from η_{plane} without trapping potential.

E: \mathbb{Z}_2 INDEX AND NUMBER EQUATION

In this section, we want to show that the measurement of number of density in momentum space can reveal the topological property of the bulk. In general, Hamiltonian has the following form under Majorana bases,

$$H_{MF} = \frac{i}{4} \sum_{\mathbf{k}} \sum_{i,j} \gamma_i(-\mathbf{k}) B_{i,j}(\mathbf{k}) \gamma_j(\mathbf{k}) \tag{31}$$

In addition to count the winding number, the condition for non-trivial TO can be revealed as \mathbb{Z}_2 index, which is Majorana number \mathcal{M} ,

$$\begin{aligned}
\mathcal{M} &= \text{sgn} [Pf(B(k_z = 0))] \text{sgn} [Pf(B(k_z = \pi/d))] \\
&= \text{sgn} [\xi_{\mathbf{k}}(k_z = 0)] \text{sgn} [\xi_{\mathbf{k}}(k_z = \pi/d)],
\end{aligned} \tag{32}$$

Here $\xi_{\mathbf{k}} = \frac{\mathbf{k}_{\parallel}^2}{2m} - \mu - 2t_z \cos(k_z)$ and Pf is the Pfaffian for antisymmetric matrix. When topology is non-trivial, then $\mathcal{M} = -1$, representing for existence of unpaired MFs in the edge surface, and $\xi_{\mathbf{k}}$ at $k_z = 0$ and $k_z = \pi/d$ must have different sign. In contrast, when $\mathcal{M} = 1$, where is no TO in the system with the same sign of $\xi_{\mathbf{k}}$ at $k_z = 0$ and $k_z = \pi/d$.

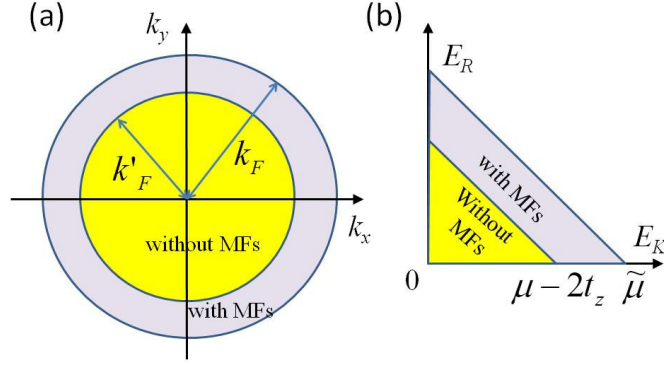


FIG. 1: The Fermi surface for polar molecules in the top or bottom layers (a) without trapping potential and (b) with harmonic trapping potential (under local density approximation). The pink (outer) regime is Kitaev's chain with unpaired MFs, while the yellow (inner) regime denotes chains without unpaired MFs. $k_F \equiv \sqrt{2m\mu}$ and $k_{Min} \equiv \sqrt{2m(\mu - 2t_z)}$ in (a). $\tilde{\mu} \equiv \sqrt{\mu^2 + 2t_z^2}$ in (b).

In zero temperature, number equation is given as $n_{\mathbf{k}} = \frac{1}{2} \left[1 - \frac{\xi_{\mathbf{k}}}{E_{\mathbf{k}}} \right]$. When $k_z = 0$ or $k_z = \pi/d$ the gap is closing, the number equation becomes

$$n_{\mathbf{k}} = \frac{1}{2} \left[1 - \frac{\xi_{\mathbf{k}}}{|\xi_{\mathbf{k}}|} \right]. \quad (33)$$

On the one hand, when $\xi_{\mathbf{k}}$ has positive sign, $n_{\mathbf{k}} = 0$. On the other hand, when $\xi_{\mathbf{k}}$ has negative sign, $n_{\mathbf{k}} = 1$. For two quantum number $k_z = 0$ or $k_z = \pi/d$, the topological non-trivial condition implies that one of the quantum states should be occupied and the other should leave empty. When system is topological trivial, both quantum states should be occupied or unoccupied. Those argument shows that the topological properties can be measured by number of density in momentum space.

[1] C.K. Chiu, J.C.Y. Teo, A.P. Schnyder, S. Ryu - Rev. Mod. Phys. 88, 035005, - APS (2016)